

Particle-hole symmetry breaking in a spin-dimer system TlCuCl_3 observed at 100 T

X.-G. Zhou,^{1,*} Yuan Yao,^{1,†} Y. H. Matsuda,^{1,‡} A. Ikeda,¹ A. Matsuo,¹ K. Kindo,¹ and H. Tanaka²

¹*Institute for Solid State Physics, University of Tokyo, Kashiwa, Chiba 277-8581, Japan*

²*Department of Physics, Tokyo Institute of Technology, Tokyo 152-8551, Japan*

The entire magnetization process of TlCuCl_3 has been experimentally investigated up to 100 T employing the single-turn technique. The upper critical field H_{c2} is observed to be 86.1 T at 2 K. A convex slope of the M - H curve between the lower and upper critical fields (H_{c1} and H_{c2}) is clearly observed, which indicates that a particle-hole symmetry is broken in TlCuCl_3 . By quantum Monte Carlo simulation and the bond-operator theory method, we find that the particle-hole symmetry breaking results from strong inter-dimer interactions.

PACS numbers: 75.10.Jm, 75.40.Cx, 75.60.Ej

Bose-Einstein condensation (BEC) is one of the most fascinating purely quantum-mechanical phenomena. Early experiments had successfully realized the BEC state on dilute atomic gas system under nanokelvin temperatures with the laser cooling technique [1]. The fact that nanokelvin temperatures is required makes experimental studies of BEC difficult to conduct and the number of the researches is limited. On the other hand, based on a correspondence between a quantum antiferromagnet and a lattice Bose gas system [2], the new research area on BEC with spin (s) systems in which spins are strongly correlated to each other, has been opened up in recent two decades. It has been proposed that the field-induced ordering phase in TlCuCl_3 (a three-dimensional $s=1/2$ spin-gap dimer system) can be interpreted as a BEC phase of magnons [3–7], and its magnetic field-temperature (H - T) phase boundary is claimed to follow the power-law dependence as,

$$g|H_{c1}(T) - H_g| \propto T^\alpha, \quad (1)$$

where g is the g -factor of the spin system, H_{c1} is one of the critical magnetic fields of the BEC at a finite temperature T , H_g is the critical magnetic field at zero kelvin, and the critical exponent $\alpha = 1.5$ under Hartree-Fock-Popov (HFP) approximation. It also provides a new experimental approach to study the BEC, i.e., magnons in three-dimensional spin-gap dimer system are studied as bosons in a lattice system.

In contrast to the ultra-cooling atomic gas, observations of critical behaviors around quantum critical points in the spin systems are accessible because of their high degree of homogeneity in boson density and wide temperature window of the critical boundary [8]. In a pure dimer system, the transition between singlet state and the $S_z = 1$ -triplet state under an external magnetic field drives a phase transition at the critical magnetic field

$H_g \equiv \Delta/g\mu_B$ with Δ the spin gap. The H_g separates into two distinct critical points H_{c1} and H_{c2} in real spin-gap materials due to inter-dimer interactions; these two critical magnetic fields correspond to the beginning and saturation of the magnetization, respectively. The criticality in the vicinity of the H_{c1} along the H - T phase boundary has been extensively studied in several materials such as TlCuCl_3 , $\text{Ba}_3\text{Cr}_2\text{O}_8$ and $\text{Sr}_3\text{Cr}_2\text{O}_8$, by means of magnetization, magnetostriction, neutron, and magnetocaloric effect (MCE) measurements [9–14]. On the other hand, detailed experimental measurements at the high-field side near H_{c2} are still lacking for materials that possess large H_{c2} like TlCuCl_3 .

In the theoretical analyses on H_{c2} of $\text{BaCuSi}_2\text{O}_6$ [15], the transformation from a spin Hamiltonian to an effective hard-core boson model was derived by projecting the original spin states to the low-energy singlet and the $S^z = 1$ -triplet states. Here, the singlet and $S^z = 1$ -triplet states, respectively, correspond to the holes (particles) and particles (holes) of bosons at a low (high) magnetic field. A particle-hole symmetry [16] in this formulation is explicit in that the effective Hamiltonians at the low magnetic field and the high field are related by a particle-hole transformation on the bosonic creation operators and, thus, the magnetic-field dependence of the order parameters in phase diagrams has a symmetry with respect to the particle-hole invariant point $H = (H_{c1} + H_{c2})/2$. For instance, such a symmetry is reflected by the mirror symmetry observed in the shape of the phase boundary of the BEC phase in $\text{BaCuSi}_2\text{O}_6$. Actually, the symmetric nature is verified in the bond operator theory [17] by showing equality of the critical exponents in the vicinity of the two critical points, H_{c1} and H_{c2} . Similar symmetric phase diagram was also obtained in $\text{Ba}_3\text{Cr}_2\text{O}_8$ [13]. In the following discussion, we will call such a *phase-diagram* symmetry as “particle-hole symmetry”.

It should be noted that the critical behaviors near the H_{c2} in the system of which inter-dimer interactions are strong has never been well investigated. In such systems, the particle-hole symmetry of the BEC phase boundary is expected to be broken because the conditions of the hard-core boson picture are not satisfied due to the effect

* zhou@issp.u-tokyo.ac.jp

† smartyao@issp.u-tokyo.ac.jp

‡ ymatsuda@issp.u-tokyo.ac.jp

of the hybridization between the singlet and $S_z = -1, 0$ - triplets. According to the bond operator theory, the pressure effect (i.e. the changing of the inter-dimer interaction) on the phase boundary in the H - T plane is different at H_{c1} and H_{c2} [18], indicating that the symmetry can be modified by the inter-dimer interaction. TiCuCl_3 is one of the most promising materials to study the symmetry of the phase boundary and discuss the particle-hole symmetry, because it possesses strong inter-dimer interactions. H_{c1} is 5.6 T [19] and H_{c2} is theoretically predicted [20] to be about 87 T; a strong contrast of these two critical points provides us a unique situation where the degrees of the quantum hybridization between the singlet and triplet states are different between two critical points. However, H_{c2} has never been experimentally observed yet in the first-discovered magnon BEC compound, TiCuCl_3 because of technical difficulties to perform a 100-T class magnetic field experiment.

In this Letter, we study the magnetization (M) process of TiCuCl_3 up to 100 T and discuss the particle-hole symmetry breaking of the BEC phase. The particle-hole symmetry in the hard-core boson picture has been found to be broken through the quantum hybridization effect due to the strong inter-dimer interactions. H_{c2} is experimentally determined to be 86.1 T at $T \approx 2$ K that is in good agreement with the prediction by the bond-operator theory [20]. The magnetization curve (M - H curve) has a monotonous convex downward shape, which manifests the difference between the critical exponents around H_{c1} and H_{c2} and implies the absence of the particle-hole symmetry in TiCuCl_3 . We have also precisely analyzed the M - H curve with a numerical calculation based on Quantum Monte Carlo (QMC) method. The simulation shows that the ratio of an inter-dimer interaction (J_2) and the intra-dimer interaction (J), J_2/J is about 0.35, which is consistent with the results of the neutron-scattering experiment [20]. Finally, we theoretically evaluate the critical exponents at near H_{c1} and H_{c2} and discuss on the microscopic origin of the breaking of the particle-hole symmetry using a combinatorial approach of the bond-operator theory and QMC calculation.

A single crystal of TiCuCl_3 [19] was used for the experiments. The single-turn coil (STC) technique was employed to generate a pulse magnetic field of up to 110 T. The magnetization measurements have been done with a pick-up coil and an induction voltage in the magnetization process is recorded as a function of time [21, 22]. The magnetization curve is obtained by a numerical integration of the measured dM/dt signal [21, 22]. In the present work, we use a double-layer pick-up coil (the number of the turns of the coil [80 in total] is doubled from the standard number[22]) which improves the signal intensity. The magnetization signal dM/dt is obtained by subtraction of the background signal from the sample signal. Here, the background signal is obtained by a measurement without the sample and the sample sig-

nal is a measured signal with the sample. The set of the two signals is obtained by two successive destructive-field measurements. This simple manner has advantages compared to the previous sample-position-exchange manner [22] in regard to stability of the measurement position and effects from inhomogeneity of the magnetic field. A liquid helium bath cryostat with the tail part made of plastic has been used [22]; the sample was immersed in liquid helium, and a measurement temperature of 2 K was reached by reducing the vapor pressure.

Fig. 1 shows the magnetization process and the magnetic field dependence of the dM/dH at 2 K; The magnetization up to 60 T in Ref. [20] is also presented for the comparison of the M - H curves. The agreement of them is excellent. The M - H curve is obtained from the average of three independent experiments using the both up-sweep and down-sweep processes; we do not use the data of magnetization below 70 T of the down-sweep for the average because the measurement in the field-decreasing process is rather imprecise due to the field inhomogeneity [21]. We analyze the H_{c1} around 6 T using the data previously obtained with a non-destructive pulse magnet [20], because, at the beginning of destructive ultra-high magnetic field generation, a huge switching electromagnetic noise is inevitably generated for injection mega-ampere driving currents [21, 22]. The magnetization is clearly measured in fields from 30 to 100 T, exhibiting the saturation at fields exceeding 90 T.

The critical behavior is observed in the vicinity of the saturation in the dM/dH curve as shown in Fig. 1: A clear peak labeled by H_{c2} in dM/dH curve corresponds

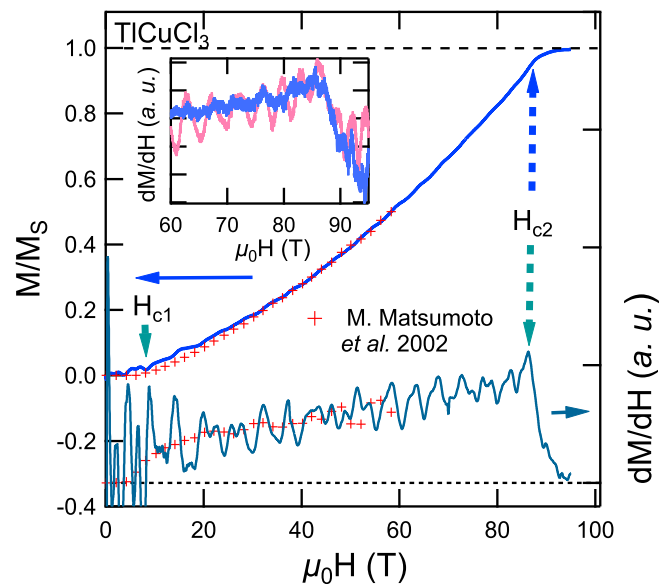


FIG. 1. (Color online) The magnetization curve measured up to 95 T, as well as the dM/dH data. Red marks represent the results of Ref. [20]. The inset shows the dM/dH data (up-sweep and down-sweep) with initial temperature at 2 K.

to a kink of the M - H curve observed at near H_{c2} . The magnetization increases continuously between H_{c1} and H_{c2} , in which the M - H curve shows a convex slope.

Due to the fast sweep rate of the pulsed magnetic field ($\sim 8 \mu\text{s}$), the sample undergoes a semi-adiabatic process. The spin entropy change caused by a phase transition is transferred into the phonons and leads to the temperature change of the sample. Therefore, it is necessary to consider the temperature change during the magnetization process. Because the MCE experiment up to 100 T is impossible to be conducted with current experimental techniques, we estimate the MCE effect using the MCE reported in another magnon BEC dimer spin system. According to Ref. [15], the temperature change at 45 T near H_{c2} in $\text{BaCuSi}_2\text{O}_6$ is around 0.03 K where the specific heat is 1.8 J/(mol K) at 2.5 K. Then entropy change $\Delta S=0.02$ J/mol is estimated to be transferred from the magnons to phonons around phase transition point. Because the entropy change in the spins at H_{c2} should reflect the way of the saturation of the magnetization where the BEC phase is terminated, the entropy change should be of more or less a similar value as other spin systems which undergo magnon BEC with spin-1/2 dimers. Therefore, the change of entropy observed in $\text{BaCuSi}_2\text{O}_6$ can be applied to the analysis on TlCuCl_3 . The specific heat in TlCuCl_3 contributed by phonons is $C_{\text{phon}}=4$ J/mol K at an initial temperature $T_{\text{in}}=2$ K [23], and thus the temperature rise from the initial temperature is estimated to be $\Delta S \cdot T_{\text{in}}/C_{\text{phon}}=0.01$ K for TlCuCl_3 at near H_{c2} . The insert of Fig. 1 shows dM/dH for both field up-sweep and down-sweep processes. The overlapping of both processes implies that the temperature variation is actually small. Thus, critical points and critical exponents can be confirmed and analyzed at 2 K in the present work.

H_{c2} is determined by the peak in the dM/dH curve and found to be 86.1 ± 0.5 T. It is very close to the predicted value obtained from the bond operator theory [20]. Furthermore, the continuous slope of the M - H curve keeps its convex shape until H_{c2} . It indicates that the critical exponents can be potentially different between H_{c1} and H_{c2} because, otherwise, it is expected that M - H curve at H_{c1} and H_{c2} should present the particle-hole symmetry behavior, i.e. the correspondences of the shapes at H_{c1} and H_{c2} are suppose to be linear versus linear, concave versus convex or convex versus concave. In order to interpret the observed magnetization process in more detail, we have tried to theoretically reproduce the M - H curve with a rather simple spin model. The lattice Hamiltonians in previous study are complex and include several types of inter-dimer interactions [18, 20]. Let us consider the following spin Hamiltonian to describe the

universality classes around H_{c1} and H_{c2} :

$$\mathcal{H}_{\text{spin}} = J \sum_{\mathbf{i}} \mathbf{S}_{\mathbf{i},1} \cdot \mathbf{S}_{\mathbf{i},2} + J_1 \sum_{\mathbf{i}} \sum_m \sum_{n=x,y} \mathbf{S}_{\mathbf{i},m} \cdot \mathbf{S}_{\mathbf{i}+\hat{e}_n,m} + J_2 \sum_{\mathbf{i}} \mathbf{S}_{\mathbf{i},2} \cdot \mathbf{S}_{\mathbf{i}+\hat{z},1} - g_{\parallel} \mu_B H \sum_{\mathbf{i},m} S_{\mathbf{i},m}^z, \quad (2)$$

where \mathbf{i} denotes the site of dimers in a cubic lattice, $m = 1, 2$ shows the position of the two spins in one dimer, $\hat{e}_n = \hat{e}_{x,y,z}$ represents the unit vector. Here J denotes the intra-dimer interaction, and $J_{1,2}$ are inter-dimer interactions in different directions. We have set two different inter-dimer interactions J_1 and J_2 , because it is necessary to fit and reproduce the experimental M - H curve in Fig. 2 and their values will be shown later. The assumed lattice for the $\mathcal{H}_{\text{spin}}$ is shown in the insert of Fig. 2. The QMC calculation is performed using a generalized directed loop algorithm in the stochastic series expansion representation [24], as implemented in the ALPS package [25]. The calculation is performed with $10 \times 10 \times 10$ unit cells, in which each unit cell contains two spin sites. Additionally, it has been reported that the structure of TlCuCl_3 is not magnetically frustrated, although the low-

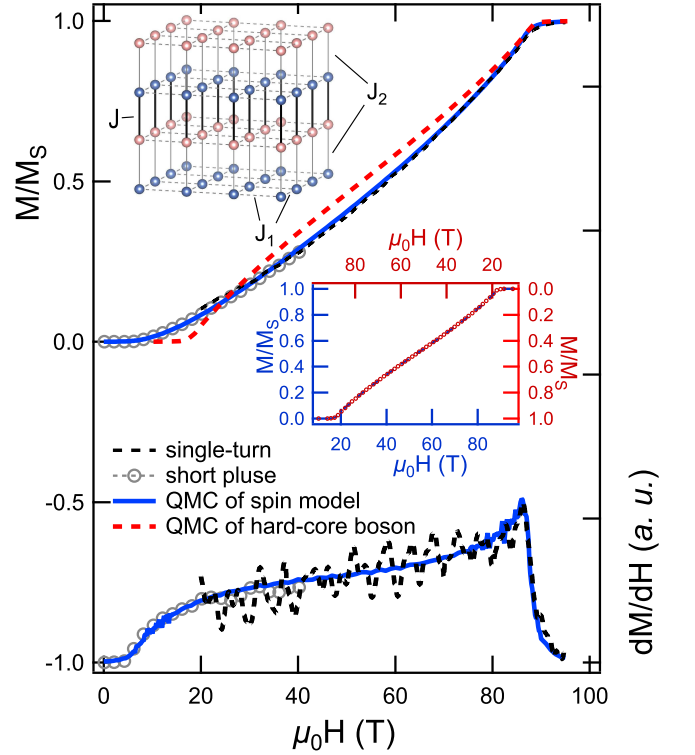


FIG. 2. Comparison between the experimental magnetization curve and the QMC simulation results, the low field data (below 40 T) is from Ref.[20], the blue and red curves is obtained from Eq. 2 and Eq. 3, respectively. The upper inset shows the lattice of spin Hamiltonian. The red and blue ball represent the spin site 1 and 2 of a dimer in Eq. (2), respectively. The middle inset shows the symmetry presentation in magnetization from Eq. 3.

symmetry structure results in many triangle interaction terms in the Hamiltonian [18].

In Fig. 2, the magnetization curves simulated by the QMC calculation are shown with the experimental data. The simulated M - H and dM/dH curves based on the Hamiltonian in Eq. (2) is represented with blue curve. The g -factor 2.23 [19] is used in this simulation. The parameters determined in this calculation are $J=5.318$ meV, $J_1=1.074$ meV and $J_2=1.86$ meV. In our reduced model, J and J_2 agree with those of the original model of TiCuCl_3 in Ref. [18, 20] according to their spin configurations. These values are also close to those reported in the previous work using the bond operator method [20]. The simulated M - H curve performed at $T = 3.5$ K is found to agree very well with the experimental magnetization process.

The hard-core boson model constructed by only the $S_z=1$ triplet and singlet states is another way to analyze the process of magnetization. Following Jaime *et al.* [15], we translate the spin Hamiltonian (Eq. 2) to an effective Hamiltonian of the hard-core boson:

$$\begin{aligned} \mathcal{H}_{\text{eff}} = & t_1 \sum_{\mathbf{i}, \alpha} (b_{\mathbf{i}+\hat{e}_n}^\dagger b_{\mathbf{i}} + b_{\mathbf{i}}^\dagger b_{\mathbf{i}+\hat{e}_n}) + t_2 \sum_{\mathbf{i}} (b_{\mathbf{i}+\hat{z}}^\dagger b_{\mathbf{i}} + b_{\mathbf{i}}^\dagger b_{\mathbf{i}+\hat{z}}) \\ & + V_1 \sum_{\mathbf{i}, \alpha} n_{\mathbf{i}} n_{\mathbf{i}+\hat{e}_n} + V_2 \sum_{\mathbf{i}} n_{\mathbf{i}} n_{\mathbf{i}+\hat{z}} + \mu \sum_{\mathbf{i}} n_{\mathbf{i}} \end{aligned} \quad (3)$$

where the chemical potential is $\mu = J - g_{\parallel} \mu_B H$, and hopping terms are $t_1 = V_1 = J_1/2$ and $t_2 = V_2 = J_2/4$. The simulation shares the same interaction parameters with the spin model. Based on this reduced model, we calculate the magnetization and show the results with the red dashed curve in Fig. 2. In contrast to the result of $\mathcal{H}_{\text{spin}}$, the magnetization derived from \mathcal{H}_{eff} shows the central symmetry that relates the magnetizations around H_{c1} and H_{c2} , which corresponds to the particle-hole symmetry shown in the middle insert of Fig. 2. However, in the following, we will see that such a symmetry is not held when the J_2 -inter-dimer interactions in Eq. (2) is significant.

As shown in Fig. 2, the magnetization gradually increases with magnetic fields when the field approaches to and exceeds H_{c1} , while the magnetization drastically changes its slope at near the saturation field H_{c2} in our experiment. This behavior can be more clearly recognized in the dM/dH curve; one can see that rather sharp peak structure appears just below H_{c2} and only a round shoulder structure is seen in the vicinity of H_{c1} . This asymmetric character of the magnetization indicates a sizable breaking of the particle-hole symmetry.

In order to clarify the asymmetric character, we utilize the following formula to perform the fitting of the magnetization.

$$|M - M_{ci}| \propto |H - H_{ci}|^{\beta_i}, \quad (i = 1, 2). \quad (4)$$

The breaking of the particle-hole symmetry can be identified by comparing two critical exponents $\beta_{1,2}$ [26] around

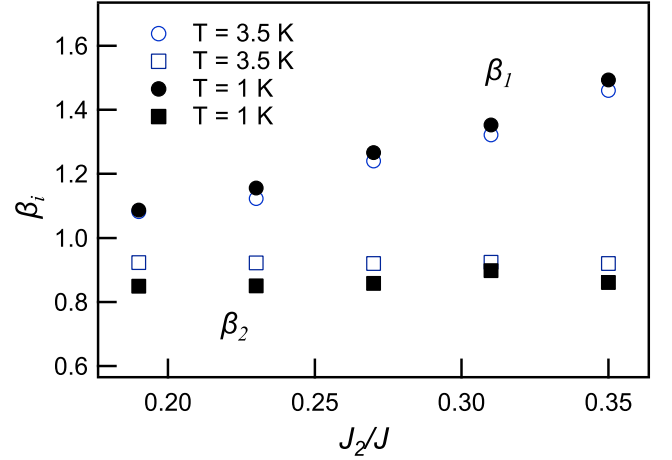


FIG. 3. β_i ($i = 1, 2$) as a function of J_2/J with fixed $J_1/J = 0.201$. The determination is performed with simulated M - H curves at 3.5 K and 1 K. Circles and squares present β_1 and β_2 , respectively.

$H_{c1,2}$ in Eq. (4) since the particle-hole symmetry implies $\beta_1 = \beta_2$.

By analyzing our experimental data with the QMC simulation, we can computationally determine the critical exponents with the simulated M - H curve [27]. We find that β_2 is robustly localized at 0.91. Here $\beta_1 \sim 1.4$ is also obtained in the same analysis but using the experimental results obtained with a non-destructive magnetic field [20]. The amount of the difference between β_1 and β_2 directly measures the degree of the asymmetry, and the difference has been found to depend on the degree of the inter-dimer coupling (itinerancy of the triplons). We have conducted an analysis of the dependence of the exponents $\beta_{1,2}$ on the inter-dimer exchange interaction J_2 . In the procedure for determination of $\beta_{1,2}$, we define field windows $x_{1,2} = (H - H_{c1,2})/(H_{c2} - H_{c1})$ which the data used should be within [11]. Accuracy of fitting process can be confirmed by stability of the obtained value when we change the field window. The fittings are performed under $x_{1,2} = 0.1, 0.15$ and 0.2 . All the obtained exponents are plotted as a function of J_2/J in Fig. 3. The range of J_2/J is set from 0.18 to 0.35. As shown in Fig. 3, β_1 gradually increases with J_2/J while the value of β_2 is more robust. The resulted J_2 -variations of β_1 and β_2 show similar behavior at 3.5 K and 1 K, indicating that the qualitative dependence of the critical exponents on the effects of the inter-dimer interaction is not affected by changing temperature from 1 to 3.5 K.

The differences between β_1 and β_2 are reflected by the convex slope of the magnetization around H_{c1} and H_{c2} as in Fig. 2; the initial magnetization process is suppressed compared to a linear magnetization while the slope increases when approaching the saturation, resulting in the larger β_1 than β_2 .

In the bond operator theoretical formalism, the mag-

netism around H_{c1} is contributed by the outset of lowest-triplet $|\uparrow\uparrow\rangle$, namely $S_z = 1$ -condensations driven by the vanishing spin gap. In the pure-dimer limit $J \gg J_{1,2}$, the other two higher-energy local excitations ($|\uparrow\downarrow\rangle + |\downarrow\uparrow\rangle$) and $|\downarrow\downarrow\rangle$ can be neglected since they hardly affect the low-temperature physics. However, a finite J_2 interaction can mediate a four-particle interaction that accumulates highest-triplet $|\downarrow\downarrow\rangle$ excitations in the presence of a partial lowest-triplet condensation and singlet condensation [18]. Therefore, $|\downarrow\downarrow\rangle$ excitations suppress the magnetization from the $|\uparrow\uparrow\rangle$ condensations when $H \gtrsim H_{c1}$. When the magnetic field increases beyond H_{c1} , such a suppression eventually becomes inefficient due to a large Zeeman gap to excite a $|\downarrow\downarrow\rangle$ quasiparticle and is negligible near H_{c2} . Therefore, we have the increasing deviation of β_1 from β_2 as shown in Fig. 3. The convex shape of the M - H curve at around H_{c1} can be understood in the same way. Moreover, it is found that β_2 is consistently insensitive to a changing of J_2/J . In short, the deviation of β_1 from β_2 is attributed to the strength of J_2 -inter-dimer interactions. Therefore, it can be concluded that the particle-hole symmetry in the hard-core boson picture (Eq. 3) is broken in TiCuCl_3 due to the strong higher-order terms through the inter-dimer interactions. Here, it should be noted that the similar inter-dimer effect is also obtained by increasing J_1 instead of J_2 . The hybridization of the four-particle states becomes relevant when J_1 or J_2 (or both) is (are) sufficiently large.

Such a particle-hole symmetry breaking has been observed in another spin-1/2 dimer system [28]. In that case, the origin of the asymmetry is claimed to be due to a zero-point quantum fluctuation characterized by the additional zero-point energy to quasi-particle excitations [29], which should be significant in low dimensional systems. However, such a quantum fluctuation in low dimensions is expected to be insignificant in TiCuCl_3 because the spin system is almost three-dimensional [30].

Furthermore, due to the insignificance of higher-energy triplet excitations around the saturation, it can be expected that the H - T phase boundary around H_{c2} obeys a power law $g|H_s - H_{c2}(T)| \propto T^\alpha$ (H_s : the saturation field strength at zero temperature) closer to the HFP approximation $\alpha = 1.5$ [3] than that regarding Eq. (1) around H_{c1} . It implies that the strong inter-dimer interactions contribute to a remarkable dispersion in the dimer spin system. This dispersion can be understood by magnon-magnon or hole-hole interaction in a boson system. Thus we have proved that the dispersion of the particle manifests itself in the asymmetric convex magnetization process, which indicates that a precise measurement of the magnetization can give us microscopic nature of magnons in some particular magnets.

In summary, we have measured the magnetization process of TiCuCl_3 at 2 K and the second critical magnetic field H_{c2} to be 86.1 T. The magnetization process shows a continuous convex slope and we analyze the critical ex-

ponents of magnetization at H_{c1} and H_{c2} . A Monte Carlo calculation based on cubic lattice well reproduces the experimental results and strongly supports the itinerant property of magnons in TiCuCl_3 . The particle-hole symmetry has been revealed to be broken in TiCuCl_3 . We have also found that the degree of asymmetry of magnetization process increases with the inter-dimer interactions by a numerical analysis with the QMC method. Thus, such interactions play an essential role in magnetization of various spin dimer systems.

X.-G. Z thank Y. Kohama and T. Nomura for fruitful discussion. X.-G. Z. was supported by MEXT scholarship. Y. Y. was supported by JSPS fellowship. This work was partially supported by JSPS KAKENHI Grant Nos. JP19J13783 (Y. Y.).

-
- [1] W. Ketterle, D. Durfee, and D. Stamper-Kurn, *Proceedings of the International School of Physics Enrico Fermi, Course* **140**, 67 (1999).
 - [2] T. Matsubara and H. Matsuda, *Progress of Theoretical Physics* **16**, 569 (1956).
 - [3] T. Nikuni, M. Oshikawa, A. Oosawa, and H. Tanaka, *Phys. Rev. Lett.* **84**, 5868 (2000).
 - [4] G. Misguich and M. Oshikawa, *Journal of the Physical Society of Japan* **73**, 3429 (2004).
 - [5] F. Yamada, T. Ono, H. Tanaka, G. Misguich, M. Oshikawa, and T. Sakakibara, *Journal of the Physical Society of Japan* **77**, 013701 (2008).
 - [6] A. Rakhimov, E. Y. Sherman, and C. K. Kim, *Phys. Rev. B* **81**, 020407 (2010).
 - [7] E. Y. Sherman, P. Lemmens, B. Busse, A. Oosawa, and H. Tanaka, *Phys. Rev. Lett.* **91**, 057201 (2003).
 - [8] T. Giamarchi, C. Ruegg, and O. Tchernyshyov, *NAT. Phys.* **4**, 198 (2008).
 - [9] N. Johansson, A. Vasiliev, A. Oosawa, H. Tanaka, and T. Lorenz, *Phys. Rev. Lett.* **95**, 017205 (2005).
 - [10] H. Tanaka, A. Oosawa, T. Kato, H. Uekusa, Y. Ohashi, K. Kakurai, and A. Hoser, *Journal of the Physical Society of Japan* **70**, 939 (2001).
 - [11] O. Nohadani, S. Wessel, B. Normand, and S. Haas, *Phys. Rev. B* **69**, 220402 (2004).
 - [12] N. Kawashima, *Journal of the Physical Society of Japan* **74**, 145 (2005).
 - [13] A. A. Aczel, Y. Kohama, M. Jaime, K. Ninios, H. B. Chan, L. Balicas, H. A. Dabkowska, and G. M. Luke, *Phys. Rev. B* **79**, 100409 (2009).
 - [14] A. A. Aczel, Y. Kohama, C. Marcenat, F. Weickert, M. Jaime, O. E. Ayala-Valenzuela, R. D. McDonald, S. D. Selesnic, H. A. Dabkowska, and G. M. Luke, *Phys. Rev. Lett.* **103**, 207203 (2009).
 - [15] M. Jaime, V. F. Correa, N. Harrison, C. D. Batista, N. Kawashima, Y. Kazuma, G. A. Jorge, R. Stern, I. Heinmaa, S. A. Zvyagin, Y. Sasago, and K. Uchinokura, *Phys. Rev. Lett.* **93**, 087203 (2004).
 - [16] F. Mila, *Eur. Phys. J. B* **6**, 201 (1998).
 - [17] H.-T. Wang, B. Xu, and Y. Wang, *Journal of Physics: Condensed Matter* **18**, 4719 (2006).
 - [18] M. Matsumoto, B. Normand, T. M. Rice, and M. Sigrist,

- Phys. Rev. B* **69**, 054423 (2004).
- [19] A. Oosawa, M. Ishii, and H. Tanaka, *Journal of Physics: Condensed Matter* **11**, 265 (1999).
 - [20] M. Matsumoto, B. Normand, T. M. Rice, and M. Sigrist, *Phys. Rev. Lett.* **89**, 077203 (2002).
 - [21] Y. H. Matsuda, N. Abe, S. Takeyama, H. Kageyama, P. Corboz, A. Honecker, S. R. Manmana, G. R. Foltin, K. P. Schmidt, and F. Mila, *Phys. Rev. Lett.* **111**, 137204 (2013).
 - [22] S. Takeyama, R. Sakakura, Y. H. Matsuda, A. Miyata, and M. Tokunaga, *J. Phys. Soc. Jap.* **81**, 014702 (2012).
 - [23] A. Oosawa, H. A. Katori, and H. Tanaka, *Phys. Rev. B* **63**, 134416 (2001).
 - [24] F. Alet, S. Wessel, and M. Troyer, *Phys. Rev. E* **71**, 036706 (2005).
 - [25] A. Albuquerque, F. Alet, P. Corboz, P. Dayal, A. Feiguin, S. Fuchs, L. Gamper, E. Gull, S. Gürtler, A. Honecker, R. Igarashi, M. Körner, A. Kozhevnikov, A. Läuchli, S. Manmana, M. Matsumoto, I. McCulloch, F. Michel, R. Noack, G. Pawłowski, L. Pollet, T. Pruschke, U. Schollwöck, S. Todo, S. Trebst, M. Troyer, P. Werner, and S. Wessel, *Journal of Magnetism and Magnetic Materials* **310**, 1187 (2007), proceedings of the 17th International Conference on Magnetism.
 - [26] Here, the critical exponents $\beta_{1,2}$ mean the the high-order term of variation, and considered to be “effective” critical exponent.
 - [27] S. Hayashida, D. Blosser, K. Y. Povarov, Z. Yan, S. Gvasaliya, A. N. Ponomaryov, S. A. Zvyagin, and A. Zheludev, *Phys. Rev. B* **100**, 134427 (2019).
 - [28] J. Brambleby, P. A. Goddard, J. Singleton, M. Jaime, T. Lancaster, L. Huang, J. Wosnitzer, C. V. Topping, K. E. Carreiro, H. E. Tran, Z. E. Manson, and J. L. Manson, *Phys. Rev. B* **95**, 024404 (2017).
 - [29] Y. Kohama, A. V. Sologubenko, N. R. Dilley, V. S. Zapf, M. Jaime, J. A. Mydosh, A. Paduan-Filho, K. A. Al-Hassanieh, P. Sengupta, S. Gangadharaiah, A. L. Chernyshev, and C. D. Batista, *Phys. Rev. Lett.* **106**, 037203 (2011).
 - [30] Because the rate of magnetic susceptibility between H_{c1} (5.6 T) and H_{c2} (86.1 T), i.e. χ_1/χ_2 in TlCuCl_3 is as large as 5 (see Fig. 1) which is 2.5 times larger than that of $\text{NiCl}_2\cdot 4\text{C}(\text{NH}_2)_2$ Ref. [29], the renormalized mass m^* is expected to be reduced by a factor of $(2.5)^{3/2} \sim 4$ compared to the case of Ref. [29]. Therefore the m/m^* in TlCuCl_3 should be as large as $3 \times 4 \sim 12$. This seems to be too large for 3-dimensional spin system TlCuCl_3 , and thus the quantum fluctuation may not be the origin of the asymmetry in TlCuCl_3 .